

ANALYTICAL AND NUMERICAL MODELING OF PASSIVE MAGNETIC BEARINGS

Nicolae TĂNASE^{1,2}, Alexandru M. MOREGA², Cristinel ILIE¹, Ionel CHIRIȚĂ¹,
Adrian NEDELCU¹, Marius POPA^{1,2}

The paper presents the theoretical aspects of passive magnetic bearings (PMBs), the analytical computation and numerical simulation of four cases for PMB with NdFeB permanent magnets in order to obtain the stiffness and magnetic forces for different static displacements of ring shape magnets. Also in this paper it is presented a comparison between the two computational methods with the results of the relative errors that have been obtained. The static numerical simulations of passive magnetic bearings (PMBs) and analytical computation make the object of this paper.

Keywords: passive magnetic bearing, static forces, static torques, permanent magnets, mechanical stiffness

1. Introduction

Magnetic bearings and their usage can be considered a topical issue in the field of active magnetic bearings (AMB) and passive magnetic bearings (PMB). Compared to classic sliding or rolling bearings with mechanical contact, AMBs and PMBs have a number of unquestionable advantages: they do not require mechanical contact, lubrication, maintenance, and they can support large loads at high peripheral speeds. These qualities imposed themselves in many top industrial sectors, such as high-performance rotary machines construction [1-5].

Magnetic bearings are suspension devices mainly used for applications that have rotating elements, but there are also applications with translational motion. The major interest for these magnetic bearings is that they are contactless, *i.e.*, there is no contact (hence no friction) between the rotating part and its support. Consequently, these magnetic bearings may work at very high rotational speeds. Passive bearings with two interacting permanent magnets can be either radial or axial. Both of them are constructed using radially and axially magnetized permanent magnets, *e.g.*, Fig. 1.

¹ Eng., Dept. of Electromechanical Systems and Technologies, National Institute for R&D in Electrical Engineering ICPE-CA, Romania, e-mail: nicolae.tanase@icpe-ca.ro

² Prof., Faculty of Electrical Engineering, University POLITEHNICA of Bucharest, ROMANIA, and the Institute of Statistical Mathematics and Applied Mathematics, the Romanian Academy, e-mail: amm@iem.pub.ro

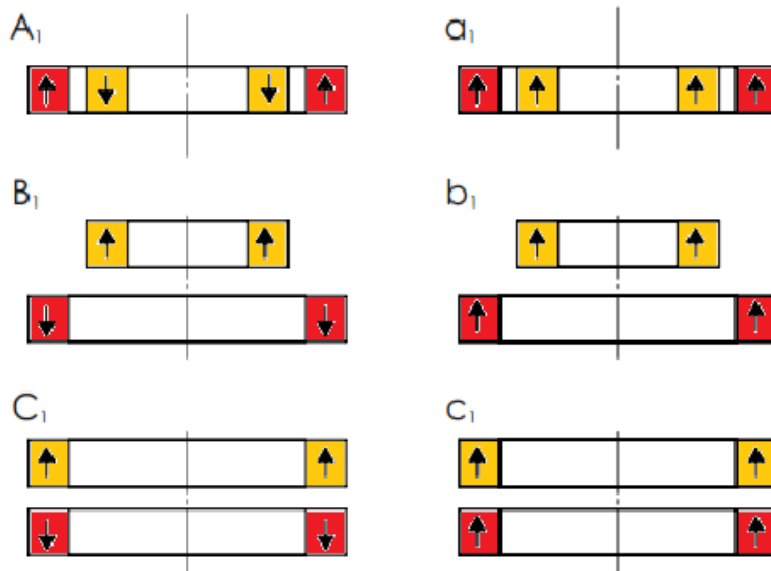


Fig. 1. Basic configurations for PMBs. The arrows indicate the direction of permanent magnetization.

2. Analytical calculation of forces and rigidity for PMBs

The high energy, NdFeB permanent magnets in the PMBs addressed in this study have the following characteristics:

- remanent magnetic flux density: $B_r = 1.3$ T;
- magnetic field strength: $H_C = 1.050 \times 10^6$ A/m;
- maximum size: 90 mm \times 90 mm \times 10 mm;
- maximum magnetic energy 40 MGs;
- the temperature is not to exceed 150 °C.

PMB structures with coaxial annular magnets are envisaged, with one or more of each of the two fixed or movable armatures of the axial and radial bearings.

In the case of interacting center magnets, the interaction parameters refer to forces and stiffnesses (interacting forces at the relative equilibrium of the magnetic rings) in axial and radial directions, respectively, which act upon them and, respectively, on the armatures which support them. The mathematical model presented in [6] is applicable to PMB systems with axial symmetry, with two coaxial cylindrical permanent magnets (in this case, ring-shaped), under the following hypotheses:

- a) there are no ferromagnetic media (closure yokes and parts);
- b) the magnets are cylindrical, with constant cross-sectional dimensions,

co-axially positioned; their axial dimensions are very large with respect to dimensions of the gap between the magnets;

- c) the magnetic polarization vectors are constant, perpendicular to the longitudinal axis;
- d) the magnetic media present high stiffness of magnetic polarization, which is practically constant in the operation, a requirement that is fulfilled by rare earths permanent magnets and hard ferrite.

The calculation of the forces and stiffness for passive magnetic bearings aims to optimize the sizing of the magnetic rings that usually form such magnetic bearings, in order to obtain maximum forces or stiffness (in accordance with the air gap). The paper aims to optimize the construction of magnetic bearings with permanent magnets, by developing a calculation model, the result of which will be compared with numerical simulations. The analytical evaluations of the magnetic forces and structural stiffness [7,8] for two center-ring magnet systems refers to the PMB sketch presented in Fig. 2.

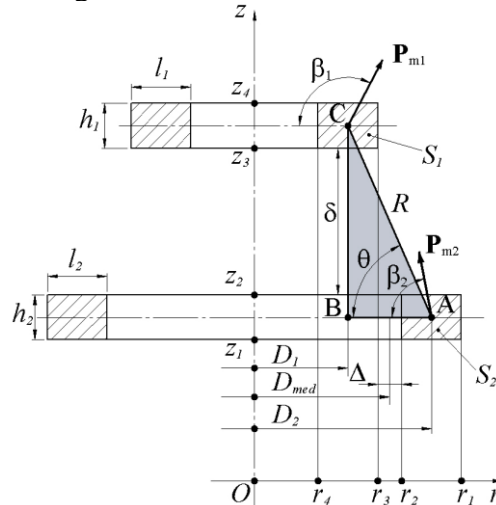


Fig. 2. Cross-sectional view of an axial-symmetric permanent magnet bearing.

Here, the cross-sectional areas of the ring magnets are $S_1 = l_1 \cdot h_1 = (r_3 - r_4)(z_4 - z_3)$; $S_2 = l_2 \cdot h_2 = (r_1 - r_2)(z_2 - z_1)$, the Euclidian distance between the magnets is $R = \sqrt{BC^2 + AB^2}$, $BC = \frac{h_1 + h_2}{2} + \delta$,

$AB = \frac{l_1 + l_2}{2} + \Delta$, δ [mm] is the size of the vertical gap between the two magnets, and Δ [mm] is the horizontal gap between them. The average perimeter of the system is $p = 2 \cdot \pi \cdot D_{med}$, where D_{med} [mm] is the average radial distance between magnets.

The analytical form of the axial magnetic force is [6]

$$F_a = p \frac{\mathbf{P}_{m1} \mathbf{P}_{m2}}{\pi \mu_0} \cdot \frac{S_1 S_2}{R^3} \cdot \sin(\beta_1 + \beta_2 - 3\theta) \text{ [N]}, \quad (1)$$

where $\mu_0 = 4\pi \cdot 10^{-7}$ H/m is the magnetic permeability of the free space, $\mathbf{P}_{m1}, \mathbf{P}_{m2}$ [T] are the permanent magnetic polarizations, $\beta_1, \beta_2 \in [0, 2\pi]$ are the magnetization angles, and $\theta \in \left[-\frac{\pi}{2}, \frac{\pi}{2}\right]$ is the angle between R and Or axis.

As the rings are centered, the radial force is

$$F_r = 0 \text{ N}, \quad (2)$$

the stiffness in the axial direction is described by

$$K_a = -2K_r = 3p \frac{\mathbf{P}_{m1} \mathbf{P}_{m2}}{\pi \mu_0} \cdot \frac{S_1 S_2}{R^4} \cdot \cos(\beta_1 + \beta_2 - 4\theta) \text{ [N/m]}, \quad (3)$$

and the stiffness in the radial direction is

$$K_r = -\frac{1}{2} K_a \text{ [N/m].} \quad (4)$$

Depending on the structure, dimensions and magnetization direction, the interaction parameters may have positive or negative values, resulting in either rejection or attraction forces, and either stable or unstable equilibrium states. Whereas for structures with two interacting ring magnets numerical simulations provide information comparative to the analytical calculations, for structures with more than two interacting permanent magnets only using numerical simulations, the results can be obtained. It is worth mentioning that, in order to obtain information regarding the stiffness (especially radial) by using analytical and numerical simulation, the ring-shaped magnets were displaced from the center position with a lower value of the eccentricity (between 0 and 1 mm).

This paper presents four cases of PMB. In Case 1 two ring magnets are used for the axial and Case 2 radial magnetic bearings. In Case 3 and Case 4 the PMB structure shows off two concentric magnets, where in Case 4 the concentric magnets represent the configuration for axial magnetic bearing. The sizes and directions of magnetizations of the permanent magnets are given in Table 1, together with the analytical results. Table 1 shows that the analytical results suggest that the axial force for Case 1 has as effect a rejection between rings, magnetic levitation. The stiffness in axial direction maintains the axial PMB in an equilibrium position. In what concerns the radial stiffness, its effect is the displacement from the equilibrium position of the PMB.

For Case 2 (radial PMB) the effect of the axial force is the attraction between the magnets. The stiffnesses in axial and radial direction are opposite as compared to Case 1. For Cases 3 and 4 there is no interaction between the rings,

no axial force, and - as in Cases 1 and 2 - the axial and radial stiffnesses have the same effects for both radial and axial PMBs.

Table 1
Analytical 2D models and results for Cases 1 to 4

Analytical 2D Model [mm]	Analytical computation results
Case 1 	$\beta_1 + \beta_2 - 3\theta = \pi/2; \beta_1 + \beta_2 - 4\theta = 0$. Axial force, $F_a = 623$ N; Axial stiffness, $K_a = 15.566 \times 10^4$ N/m; Radial stiffness, $K_r = -7.783 \times 10^4$ N/m.
Case 2 	$\beta_1 + \beta_2 - 3\theta = \pi/2; \beta_1 + \beta_2 - 4\theta = 0$. Axial force, $F_a = -396.62$ N; Axial stiffness, $K_a = -4.2335 \times 10^4$ N/m; Radial stiffness, $K_r = 2.1167 \times 10^4$ N/m.
Case 3 	$\beta_1 + \beta_2 - 3\theta = \pi; \beta_1 + \beta_2 - 4\theta = \pi$. Axial force, $F_a = 0$ N; Axial stiffness, $K_a = -10.244 \times 10^4$ N/m; Radial stiffness, $K_r = 5.122 \times 10^4$ N/m.
Case 4 	$\beta_1 + \beta_2 - 3\theta = 0; \beta_1 + \beta_2 - 4\theta = 0$. Axial force, $F_a = 0$ N; Axial stiffness, $K_a = 10.244 \times 10^4$ N/m; Radial stiffness, $K_r = -5.122 \times 10^4$ N/m.

3. Numerical simulation of PMB systems

The PMB magnetostatic models are solved numerically using FEM [9]. The computational domain is contained in a cylinder with a radius $R = 45$ mm so that the boundary is conveniently far away from the magnetic field source. The remanent magnetic flux density is $B_r = 1.2$ T. The magnetic field is described by [9,10]

$$-\nabla(\mu_0\mu_r\nabla V_m - \mathbf{B}_r) = 0, \quad (5)$$

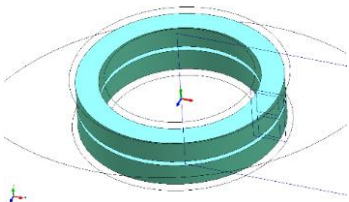
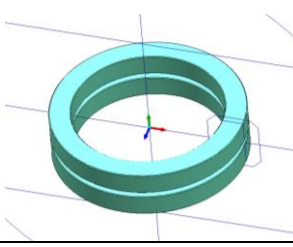
where V_m [A] is the scalar magnetic potential, μ_0 is the magnetic permeability of the free space, μ_r is the relative magnetic permeability ($\mu_r = 1.03967$ for magnets and other components of the passive magnetic bearing). Magnetic insulation boundary condition

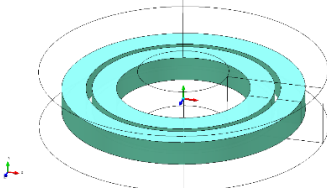
$$\mathbf{n} \cdot \mathbf{H} = 0 \Rightarrow \frac{\partial V_m}{\partial n} = 0, \quad (6)$$

where \mathbf{n} is the outward normal to the boundary, closes the problem. The 3D models and sizes of the four PMBs are presented in Table 2.

Table 2

The 3D models for numerical simulations Cases 1 to 4

3D Models	Dimensions (see Fig. 2 for notation)
Case 1 	$D_{ext} = \emptyset 90$ mm; $h_1 = l_1 = h_2 = l_2 = 10$ mm; $\delta = 2$ mm.
Case 2 	$D_{ext} = \emptyset 80$ mm; $h_1 = l_1 = h_2 = l_2 = 8$ mm; $\delta = 2$ mm.
3D Models	Dimensions (see Fig. 2 for notation)

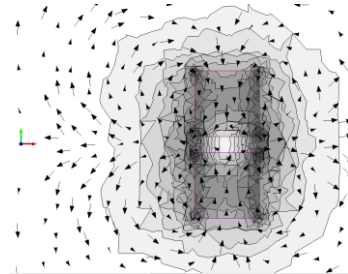
Cases 3 and 4

$$D_{ext} = \emptyset 80 \text{ mm};$$

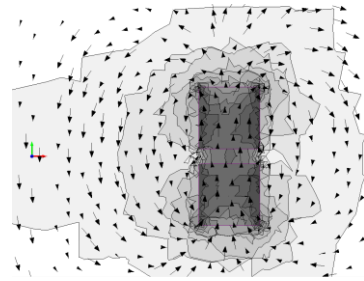
$$h_1 = l_1 = h_2 = l_2 = 8 \text{ mm};$$

$$\delta_x = \delta_y = 2 \text{ mm}.$$

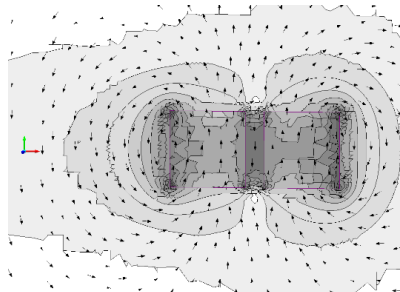
The FEM mesh consists of *approx.* 280,000 tetrahedral elements, which is a finer mesh, according to a usual computing power, used for accurate results. In the air gap between the magnets, the mesh was finer. The magnetic field spectra for Cases 1 to 4 are shown in Fig. 3.



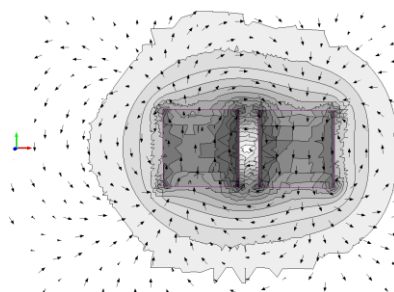
a) Case 1 - $|\mathbf{B}_{\max}| = 1.383 \text{ T}$;



b) Case 2 - $|\mathbf{B}_{\max}| = 1.420 \text{ T}$;



c) Case 3 - $|\mathbf{B}_{\max}| = 1.499 \text{ T}$;



d) Case 4 - $|\mathbf{B}_{\max}| = 1.611 \text{ T}$.

Fig. 3. Magnetic field spectra of the PMBs.

Static axial magnetic forces and torques for Cases 1 and 2 and the radial magnetic forces *w.r.t.* the radial displacement for Cases 3 and 4 were obtained through numerical simulations. The static axial and radial stiffnesses for Cases 1 to 4 were obtained from numerical simulations. Table 3 presents the numerical simulation results for axial static magnetic forces and torques for Case 1, for $\delta = 2 \text{ mm}$.

Table 3

Magnetic forces and torques for concentric ring structure magnets, in Case 1 for $\delta = 2 \text{ mm}$									
	Axial magnetic force [N]				Magnetic torque [Nm]				module
	X	Y	Z	module	X	Y	Z	module	
Upper magnet	-0.104	576	0.353	576	0.0091	-0.0008	-0.0091	0.0129	
Lower magnet	-0.168	-576	-0.087	576	0.00753	0.00046	-0.0083	0.0112	

To reduce the numerical calculation error, we will consider the average values of the program values for the two magnets. For example

$$F_{xcase} = \frac{|F_{xupper_magnet}| + |F_{xlower_magnet}|}{2} \cdot \frac{F_{xupper_magnet}}{|F_{xupper_magnet}|} \text{ [N].} \quad (7)$$

The stiffness in Ox direction is $\chi_x = -32.5 \text{ N/mm}$ and in Oy direction it is $\chi_y = 129 \text{ N/mm}$. Table 3 shows that the results for axial force, $F_a = 576 \text{ N}$, are very close to the analytical calculation, with the relative error of $\sim 8\%$ (see Table 1 for F_a).

Table 4 provides the data for numerical simulation results for axial static magnetic forces and torques for Case 2, for $\delta = 2 \text{ mm}$.

Table 4

Magnetic forces and torques for concentric ring structure magnets, in Case 2 for $\delta = 2 \text{ mm}$				
Axial magnetic force [N]	X	Y	Z	module
Upper magnet	-0.442	-341	-0.219	341
Lower magnet	0.0194	343	-0.12	343
Magnetic torque [Nm]	X	Y	Z	module
Upper magnet	0.00427	-0.0019	0.000434	0.0047
Lower magnet	0.00501	-0.0015	-0.00258	0.00583

The stiffness along Ox is $\chi_x = 44.8 \text{ N/mm}$ and along Oy is $\chi_y = -76 \text{ N/mm}$. The results in Table 4 are close to $F_a = -341 \text{ N}$, with the relative error of $\sim 14\%$ (see Table 1 for F_a).

Table 5 presents the numerical simulation results for magnetic forces for Cases 3 and 4, for $\delta = 1 \text{ mm}$.

Table 5

Magnetic forces for concentric ring shape magnets structure, in Cases 3 and 4 for $\delta = 1 \text{ mm}$

Outer magnet 1		Inner magnet 2		Displacement [m]	Direction of magnetization
Fx [N]	Fy [N]	Fx [N]	Fy [N]		
0.28	-0.358	0.0627	0.0402	[0; 0; 0]	[0; -1; 0]
0.125	-1.3	0.208	-0.889	[0; 0; 0]	[0; 1; 0]
28.5	-0.336	-28.4	-0.265	[0.0005; 0; 0]	[0; -1; 0]
-23	-1.4	22.9	-1.24	[0.0005; 0; 0]	[0; 1; 0]
55.9	-0.326	-55.4	-0.925	[0.001; 0; 0]	[0; -1; 0]
-51	-0.659	51.6	-1.48	[0.001; 0; 0]	[0; 1; 0]

Fig. 4 presents the static radial magnetic forces for Cases 3 and 4 with magnets that has the same direction of magnetization and opposite direction of magnetization of the permanent magnets.

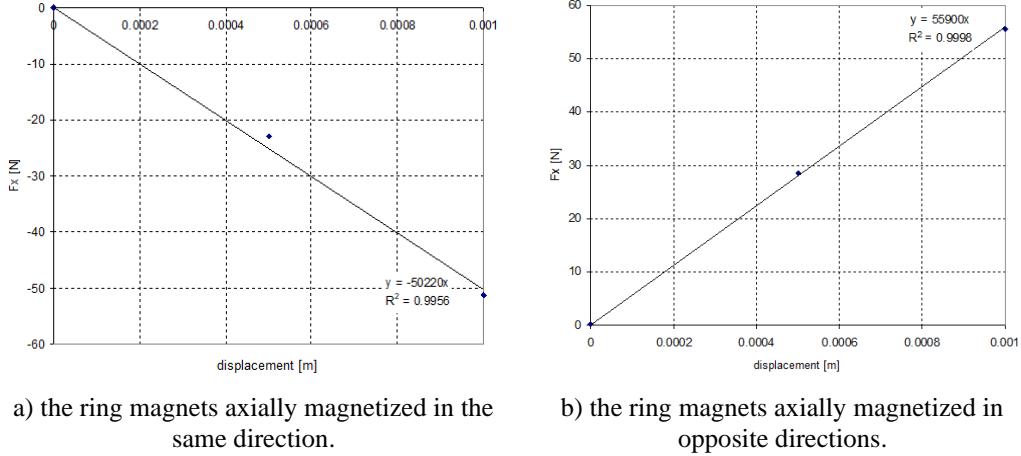


Fig. 4. Radial force in Ox direction vs. radial displacement.

The radial stiffness results obtained from Fig. 4 when the magnets have the same direction of magnetization is $\chi_x = 50$ N/mm and for opposite directions $\chi_x = 56$ N/mm. Fig. 4 shows that the radial force F_x has a linear variation *w.r.t.* the radial displacement in Ox direction. This can be explained that the tendency of the inner magnet is to self-center in the equilibrium position.

The negative and positive results depend on the direction of magnetization of the inner magnet.

4. Conclusions

Comparing the analytical and numerical results for the interaction parameters that characterize the axial and radial magnetic bearings it was found that the analytical calculation (when possible) is applicable only to centered permanent magnet systems. For Case 1, with two identical magnetic rings magnetized in opposite directions, the analytically solution for the axial force for an axial displacement of $\delta = 2$ mm is 623 N, whereas numerical simulation result is 576 N. These show off a relative error of $\sim 8\%$, considering the analytical solution as reference value. For Case 2, with two identical magnetic rings magnetized in same direction, the analytically calculated axial sustained force for an axial displacement of $\delta = 2$ mm is -396.62 N, whereas the numerical simulation result is -341 N, with a relative error being $\sim 14\%$, which is higher comparing to Case 1, because of the results obtained from numerical simulations (that is more precise, which involves several solving equations). For Cases 3 and 4 the results for the radial force was computed through numerical simulations

only, and the maximum radial force for a radial displacement of $\delta = 1$ mm is 51.6 N. On concluding, analytical solutions – when available – may be used for preliminary sizing, but the final sizing should be through numerical simulation.

R E F E R E N C E S

- [1]. *T. L. Dragomir, I. Silea*, Control system for the magnetic bearings of a balancing machine, *Journal of Electrical Engineering*, **vol. 3**, Universitatea Politehnica Timisoara, 2003.
- [2]. *G. Schweizer*, Active magnetic bearings-chances and limitations, International Centre for Magnetic Bearings, ETH Zurich, www.mcgs.ch/web, 2006.
- [3]. *E. Burzo*; Magneți permanenți (Permanent Magnets), Editura Academiei, **vol.2**, București, 1987.
- [4]. *B. Paden, N. Groom, J. F. Antaki*, Design Formulas for Permanent-Magnet Bearings, *Journal of Mechanical Design*, **vol. 125**, December 2003, pp. 734-738.
- [5]. *B. Polajžer*, Magnetic Bearings, Theory and Applications, Published by Sciendo Janeza Trdine 9, 51000 Rijeka, Croatia, ISBN 978-953-307-148-0, 2010.
- [6]. *J.P. Yonnet*; Permanent Magnet Bearings and Couplings, *IEEE Transactions on Magnetics*, **vol. MAG – 17**, nr. 1, January 1981.
- [7]. *G. Mihăiescu*, Contribuții la studiul și realizarea unor sisteme speciale cu magneți permanenți (Contributions to the study and realization of special systems with permanent magnets), Teză de Doctorat, UPB, Facultatea de Inginerie Electrică, București, 2007.
- [8]. *W. Kappel, G.M. Mihăiescu, S. Alexandru, I. Ivan, C. Iftode, H. Gavrilă, V. Ioniță*, Elemente privind transmiterea momentului mecanic fără contact între repere în mișcare de rotație, prin cuplaje cu magneți permanenți (Elements of transmission of the non-contact mechanical moment between rotating moving parts through permanent magnet couplings), Sesiunea de comunicări ARM-2, Constanța, 2001.
- [9]. *** Infolytica Corporation (Mentor Graphics) – 2D/3D Electromagnetic Field Simulation Software, 2015.
- [10]. *C.I. Mocanu*, Teoria câmpului electromagnetic (The theory of electromagnetic field), Ed. Didactică și Pedagogică, București, 1982.